

Numerical solution to the 1D grey radiation hydrodynamics equations with entropy-based artificial viscosity.

Marc-Olivier Delchini*, Jim Morel[†] and Jean C. Ragusa[‡]

December 8, 2013

*Nuclear Engineering Department Texas A&M University 3133 TAMU College Station, TX 77843-3133, delchini@tamu.edu

[†]Nuclear Engineering Department Texas A&M University 3133 TAMU College Station, TX 77843-3133, jim.morel@tamu.edu

[‡]Nuclear Engineering Department Texas A&M University 3133 TAMU College Station, TX 77843-3133, jean.ragusa@tamu.edu

Abstract

It is proposed to use an artificial viscosity method called the entropy-based viscosity method [2, 3, 12] to solve the 1D grey radiation-hydrodynamic equations. Some theoretical aspects are introduced related to the entropy minimum principle [13] in order to justify the derivation of the dissipative terms and the smart viscosity coefficient. The equations are discretized with Continuous Galerkin Finite Element Method (CGFEM) and implicit temporal integrator using the Moose framework [20]. The method of manufactured solution (MMS) is used to prove second-order accuracy for both the equilibrium diffusion and streaming limits. Then, some typical test cases for 1-D radiation hydrodynamic equations are run to demonstrate the capabilities of the entropy-based viscosity method in resolving shocks.

Keywords: second-order accuracy, artificial viscosity method, entropy-based viscosity method, implicit, radiation-hydrodynamic.

1 Introduction

Solving the radiation hydrodynamic equations is a challenging task for multiple reasons. First, the characteristic time scales between the two physics are different of several order of magnitude which often requires the radiation part to be solved implicitly to ensure stability. Second, alike any wave-dominated problems, special attention needs to be taken in order to accurately resolve shocks that may occur. Third, achieving high-order accuracy is challenging but some recent work has shown some promising results for achieving high-order accuracy both in time and space when solving Euler equations [1, 2, 3, 4] and the radiation equation independently from each other. And, fourth, the radiation hydrodynamic equations are stiff to solve in the equilibrium diffusion limit, mainly because of the relaxation source terms that couple the two physics.

A lot of effort has been put into developing a Riemann solver for both the radiation and hydrodynamic equations that accurately resolve shocks and ensure high-order convergence away from the shock region. Balsara [5] developed a Riemann solver for the radiation-hydrodynamic equations by considering the frozen approximation that decouple the two physics. However, such approach can reveal itself dangerous when solving for the equilibrium diffusion limit. In this case, the coupling terms drive the physics and have to be accounted for. Some work has been done in [6] in this direction in order to develop a *generalized Riemann solver* which accounts exactly for the relaxation terms. Another approach, when solving for the equilibrium limit, is to recast the system of equations under a conservative form. Then, a numerical solution can be obtained by modifying the equation of state. This modification is referred as the radiation-modified equation of state (REOS) and is easy to implement by taking any solver for Euler equations and replace the equation of state by the REOS [7].

As mentioned earlier, the high-order accuracy needs to be considered as well. A great amount of work is available in the literature when it comes to solve for Euler equations and the radiation transport equation [9, 8], independent to each other. However, achieving high-order accuracy when coupling the two physics is not an easy process because of the different time scales. Edwards and al. proposed a two stages semi-implicit scheme called IMEX [10]. They applied a Trapezoidal/BDF2 temporal discretization scheme to nonlinear grey radiative diffusion. The radiation and hydrodynamic equations are solved implicitly and explicitly, respectively. A Riemann solver along with flux limiter are used to resolve shocks and other waves. Results show good agreement with analytical solutions.

We now propose to solve the 1D radiation hydrodynamics equations by using *the entropy-based viscosity method*. The technique was developed by Guermond et al. for hyperbolic system of equations ([2]) and consists in adding dissipative terms in the governing equations with a second order viscosity coefficient that modulates locally the amount of dissipation. Generally speaking, entropy is produced at shocks [11]; as a result, oscillations can occur in numerical schemes. Using the entropy-based viscosity method, these oscillations can be controlled and removed by adding adequate viscosity. This method was successfully applied to non-linear hyperbolic equation using various discretization methods and achieved high-order accuracy on non-uniform meshes and complex geometries ([12, 3]).

The 1D grey radiation-hydrodynamic (GRH) equations are recalled in Eq. (1), and the corresponding variables are defined for clarity purposes:

$$\begin{cases} \partial_t (\rho) + \partial_x (\rho u) = 0 \\ \partial_t (\rho u) + \partial_x (\rho u^2 + P + \frac{\epsilon}{3}) = 0 \\ \partial_t (\rho E) + \partial_x [u (\rho E + P)] = -\frac{u}{3} \partial_x \epsilon - \sigma_a c (aT^4 - \epsilon) \\ \partial_t \epsilon + \frac{4}{3} \partial_x (u \epsilon) = \frac{u}{3} \partial_x \epsilon + \partial_x \left(\frac{c}{3\sigma_t} \partial_x \epsilon \right) + \sigma_a c (aT^4 - \epsilon) \end{cases}, \quad (1)$$

where ρ , u , E , ϵ , P and T are the material density, material velocity, material specific total energy, the radiation energy density, material pressure and temperature, respectively. The total and absorption cross-sections, σ_t and σ_a , are temperature dependent. The variables a and c are the Boltzman constant and the speed of light, respectively. Lastly, the symbols ∂_t and ∂_x denote the temporal and spatial partial derivatives, respectively. The material temperature and pressure are computed with the Ideal Gas equation of state (IGEOS):

$$\begin{cases} P = (\gamma - 1)C_v\rho T \\ e = C_v T \end{cases} \quad (2)$$

where e is the specific internal energy and computed from the expression: $e = E - 0.5u^2$. The heat capacity C_v and the heat ratio coefficient γ are assumed constant.

This paper is organized as follows: first, the entropy-based viscosity method is introduced and some detailed regarding the derivation of the dissipative terms and the viscosity coefficients are given. Then, the second-order accuracy of the scheme is proven by using the Method of Manufactured Solution (MMS) both in the equilibrium diffusion and streaming limits. Then, numerical results are shown for Mach numbers varying from 1.05 to 50.

2 The entropy-based viscosity method applied to the 1-D Radiation-Hydrodynamic equations:

In this section it is proposed to adapt the entropy-based viscosity method [12] to the 1-D Radiation-Hydrodynamic equations through a step process. First, the reader is guided through the main steps that lead to the derivation of the dissipative terms, using the entropy minimum principle [13]. Then, a definition for the entropy viscosity coefficient based upon the entropy production is given.

Let us recall here that the entropy-based viscosity method was developed for hyperbolic system of equations. The radiation hydrodynamic equations are not strictly hyperbolic but numerous numerical techniques are based on the study of the hyperbolic parts [5, 14]. Thus, following the same reasoning, the system of equations given in Eq. (1) is made hyperbolic by assuming an infinite opacity (the frozen approximation) and by not considering the relaxation terms. Thus, these two assumptions yield the following system of equations:

$$\begin{cases} \partial_t(\rho) + \partial_x(\rho u) = 0 \\ \partial_t(\rho u) + \partial_x(\rho u^2 + P + \frac{\epsilon}{3}) = 0 \\ \partial_t(\rho E) + \partial_x[u(\rho E + P)] = -\frac{u}{3}\partial_x\epsilon \\ \partial_t\epsilon + \frac{4}{3}\partial_x(u\epsilon) = \frac{u}{3}\partial_x\epsilon \end{cases} \quad (3)$$

The jacobian matrix of the hyperbolic terms can be computed to derive the eigenvalues:

$$\lambda_1 = u - c_m, \lambda_{2,3} = u \text{ and } \lambda_4 = u + c_m \quad (4)$$

where c_m is the material speed of sound and defined as follows:

$$c_m^2 = P_\rho + \frac{P}{\rho}P_e + \frac{4\epsilon}{9} \quad (5)$$

The above hyperbolic system of equation can be recast in a conservative form which allow us to assume the existence of an entropy function s [15], function of the internal energy e , the density

ρ and the energy radiation density ϵ . Then, using the chain rule (Appendix A) an equation verified by the entropy s is derived:

$$D_e(x, t) = \rho \frac{ds}{dt} = \rho (\partial_t s + u \partial_x s) = 0, \quad (6)$$

where $\frac{d}{dt}$ denotes the total or material derivatives. Eq. (6) is often referred as the entropy residual and used to prove the entropy minimum principle $\frac{ds}{dt} \geq 0$ [13].

When adding dissipative terms to each equation of Eq. (3) as stated by the entropy-based viscosity method, the entropy equation/residual gets modified since extra terms will appear in the right hand side of Eq. (6). The sign of this extra terms needs to be studied for the entropy minimum principle to hold. Thus, such a condition is used to derive an expression for each of the dissipative terms. The derivation that leads to the final expression of the dissipative terms is a long process and only the final result along with the key assumptions are given here. The reader can refer to Appendix A for details. The system of equation with the dissipative terms is the following:

$$\begin{cases} \partial_t(\rho) + \partial_x(\rho u) = \partial_x(\kappa \partial_x \rho) \\ \partial_t(\rho u) + \partial_x(\rho u^2 + P + \frac{\epsilon}{3}) = \partial_x(\kappa \partial_x \rho u) \\ \partial_t(\rho E) + \partial_x[u(\rho E + P)] + \frac{u}{3} \partial_x \epsilon = \partial_x(\kappa \partial_x(\rho E)) \\ \partial_t \epsilon + \frac{4}{3} \partial_x(u \epsilon) - \frac{u}{3} \partial_x \epsilon = \partial_x(\kappa \partial_x \epsilon) \end{cases}, \quad (7)$$

where κ is a local positive viscosity coefficient or also called vanishing viscosity coefficient. It was assumed:

$$\begin{cases} P \frac{\partial s}{\partial e} + \rho^2 \frac{\partial s}{\partial \rho} + \frac{4}{3} \rho \epsilon \frac{\partial s}{\partial \epsilon} \\ s(\rho, e, \epsilon) = \hat{s}(\rho, e) + \frac{\rho_0}{\rho} \tilde{s}(\epsilon) \end{cases} \quad (8)$$

where $-\tilde{s}$ is convex as a function of the radiation energy density ϵ and $-\hat{s}$ is convex as a function of the internal energy e and the specific volume $\frac{1}{\rho}$. The constant ρ_0 is of order one and is only here because of dimension purpose. Once the dissipative terms are derived, it remains to define the local viscosity coefficient $\kappa(x, t)$. This is not an easy task and great care needs to be taken. It is proposed to explain the reasoning that leads to a definition for the viscosity coefficient κ . The definition of the viscosity coefficient κ must meet the three following requirements:

- An upper bound is required for stability of the numerical scheme: when considering explicit temporal integrators, the maximum value of the viscosity coefficient is related to the Current Friedrich Lax number (CFL). This upper bound is defined by analogy to the upwind scheme that is known to efficiently smooth out oscillations. With implicit temporal integrators, the same reasoning is used even if the CFL number is in theory no longer required. This upper bound will be referred to as the *first order viscosity*: $\kappa_{max}(x, t)$.
- It was mentioned in this paper that the entropy residual can measure the entropy production that occurs in shock regions (the entropy residual experiences a peak). Thus, defining a viscosity coefficient proportional to the entropy residual will allow us to track the shock and also give us a measure of the viscosity required to stabilize the scheme. This viscosity coefficient is referred to as the *entropy viscosity coefficient* or *second order viscosity coefficient*: $\kappa_e(x, t)$ where the subscript e states for entropy.
- The viscosity coefficients that is actually used in the dissipative terms, κ , of Eq. (3) is defined as follows: $\kappa(x, t) = \min(\kappa_e(x, t), \kappa_{max}(x, t))$. With such a definition, the viscosity added to the system of equation will saturate to the first order viscosity in the shock region. Any where else, the entropy production will be very small so as the viscosity coefficient κ .

It remains now to define the first and second order viscosity coefficients. Following the work of Valentin and al. [12], a definition for the first order viscosity is chosen to be:

$$\kappa_{max} = \frac{h}{2} (|u| + c_m) \quad (9)$$

where h is the grid size and all other variables were defined previously. This definition was derived based on the upwind scheme and a simple derivation can be found in [2] for the case of scalar hyperbolic equation. Through the definition of the speed of sound c_m , both the material and radiation properties are accounted for in the definition of the first order viscosity coefficient. The definition of the second order viscosity coefficient, $\kappa_e(x, t)$, is to be based upon the entropy residual (Eq. (6)) that can be recast as a function of the pressure P , the density ρ and the radiation density energy ϵ (Appendix A):

$$\tilde{D}_e(x, t) = \frac{s_e}{P_e} \underbrace{\left(\frac{dP}{dt} - c_m^2 \frac{d\rho}{dt} + \frac{d\epsilon}{dt} \right)}_{\hat{D}_e(x, t)} \quad (10)$$

where $\frac{d}{dt}$ denotes the material or total derivative. s_e is defined as the inverse of the material temperature (Appendix A) and P_e is computed from the IGEOS. Those two terms are positive so that the sign of the entropy residual $\tilde{D}_e(x, t)$ can be determined by simply looking at the terms inside the brackets $\hat{D}_e(x, t)$. Such an expression is easier to compute than the one given in Eq. (6) that requires an analytical expression of the entropy function. Thus, the entropy viscosity coefficient $\kappa_e(x, t)$ is set to be proportional to $\hat{D}_e(x, t)$. Since the units of the viscosity coefficients are $m^2 s^{-1}$, a possible definition for $\kappa_e(x, t)$ would be:

$$\kappa_e(x, t) = h^2 \frac{\max(|\hat{D}_e(x, t)|, J)}{\rho c_m^2} \quad (11)$$

where J is the jump of a given quantity at cell interface. Its definition is discretization-dependent and defined as follows for CGFEM:

$$\begin{cases} J_P = |u| [[\partial_x P]] \\ J_\rho = c^2 |u| [[\partial_x \rho]] \\ J = \max(J_\rho, J_P) \end{cases} \quad (12)$$

The jumps of the pressure and density gradient are included in the definition of the viscosity coefficients since they are a good shock indicator (with CGFEM, the variables are continuous at the interface but their gradients are discontinuous). The symbol $[[\cdot]]$ denotes the jump at the interface.

The entropy-based viscosity method is now well defined for the hyperbolic system of Eq. (3) and will be used to solve the 1D grey radiation-hydrodynamic equations given in Eq. (1). Thus, we can wonder how the relaxation source terms $\sigma_a c(aT^4 - \epsilon)$ and the physical diffusive term $\partial_x(D\partial_x \epsilon)$ may affect the entropy-based viscosity method. When applying the entropy-based viscosity method, the radiation energy density equation has now a diffusive term and a numerical dissipative term with a vanishing viscosity coefficient κ . As long as the diffusive coefficient is larger than the viscosity coefficient κ , the numerical dissipative term should not be required. A way to ensure consistency and prevent the formation of the oscillations when tending to the froze in limit, is to merge the two second-order derivative terms into one as follows:

$$\partial_x \left(\frac{c}{3\sigma_t} \partial_x \epsilon \right) + \partial_x (\kappa \partial_x \epsilon) = \partial_x \left[\max \left(\frac{c}{3\sigma_t}, \kappa \right) \partial_x \epsilon \right] \quad (13)$$

Thus, as long as the artificial viscosity coefficient κ is locally smaller than the physical diffusive coefficient $D = \frac{c}{3\sigma_t}$, no artificial viscosity is required to ensure stability of the numerical scheme. As the diffusive coefficient D goes to zero, shock can form in the radiation energy density profile and will require a certain amount of viscosity in order to prevent oscillations from forming.

The effect of the relaxation source terms onto the entropy-based viscosity method can become problematic in the equilibrium diffusion limit ($\sigma_a c \rightarrow \infty$): the relaxation source terms behave as dissipative terms and make the system parabolic [4]. In [18], a study on the impact of various artificial viscosity methods onto hyperbolic system with relaxation terms is carried out. It is shown that high-order viscosity coefficients are better suitable since they do not alter the physical solution as much as first order viscosity like upwind scheme. A manufactured method solution is designed in Section 3.1 to test the convergence of the numerical solution to the equilibrium-diffusion limit.

Remark 2.1. *The coefficient ρc_m^2 is used as a normalization parameter to make the ratio $\hat{D}_e(x, t)/\rho c_m^2$ have the unit of inverse time. The normalization factor has to be larger than h in order to conserve the high-order accuracy.*

Remark 2.2. *The reader will notice that besides the definition of the jump, the whole method is independent of the numerical discretization method. It could be used with either discontinuous Galerkin finite element or finite volume methods. In both cases, a definition of the jump can be found in [12].*

3 Numerical results:

In this section, numerical results of the dimensional 1D grey radiation-hydrodynamics equations are presented using the entropy-based viscosity method. First, second order accuracy of the method is demonstrated by using the method of manufactured solution (MMS). Then, some typical test cases for radiation-hydrodynamic equations are shown. The equations are discretized using CGFEM in the Moose framework [20]. First order polynomials are used for the spatial discretization. The second-order BDF2 implicit temporal integrator is employed. The system is solved by a Preconditioned Jacobian Free Newton Krylov solver (PJFNK) where the full jacobian matrix is used as a preconditioner.

Remark 3.1. *The entropy residual is not discretized with finite element type method, but evaluated locally at the quadrature points using a finite volume type approach since the finite element discretization allows us to compute locally the spatial and temporal derivatives of any nodal quantities. The time dependent term is discretized using BDF2 or Crank-Nicolson [4].*

3.1 Method of Manufactured Solution:

The same manufactured solution as in [17] are used in order to test both the diffusive and streaming limit solutions on a slab of thickness $L = 2\pi$ cm. The manufactured solutions are composed of trigonometric function. Periodic boundary conditions are used for all of the variables. The L2 norm error between the numerical and exact solutions is computed for the density, momentum, total material energy and radiation density energy. For each new simulation, the time step is divided by two and the number of degree of freedom is doubled. With such settings, the error is expected to decrease by a factor 4.

The first manufactured solution is design to test the equilibrium diffusion limit. In that case, the

radiation energy is in equilibrium with the material temperature and the opacity is large which means that the radiation mean-free path is not resolved. The following exact solution was used:

$$\begin{cases} \rho = \sin(x - t) + 2 \\ u = \cos(x - t) + 2 \\ T = \frac{0.5\gamma(\cos(x-t)+2)}{\sin(x-t)+2} \\ \epsilon = aT^4 \end{cases} \quad (14)$$

The cross-sections σ_a and σ_t are assumed constant and set to the same value 1000 cm^{-1} . The simulation is run until $t = 3 \text{ sh}$. The L2 error norm along with the ratio between consecutive simulation are given in Table 1 for the equilibrium diffusion limit:

Table 1: Convergence study for the first manufactured solution.

DoF	$\Delta t \text{ (sh)}$	ρ	ratio	ρE	ratio	ϵ	ratio	ρu	ratio
20	10^{-1}	0.590766	NA	1.333774	NA	0.00650085	NA	0.910998	NA
40	$5 \cdot 10^{-1}$	0.290626	2.03	0.478819	2.79	0.00124983	5.20	0.4090946	2.23
80	$2.5 \cdot 10^{-2}$	0.0959801	3.021	0.154119	3.11	0.000262797	4.76	0.125943	3.25
160	$1.25 \cdot 10^{-2}$	0.02593738	3.70	0.0405175	3.80	$6.17726 \cdot 10^{-5}$	4.25	$3.381042 \cdot 10^{-3}$	3.72
320	$6.25 \cdot 10^{-3}$	$6.471444 \cdot 10^{-3}$	4.00	$9.90446 \cdot 10^{-3}$	4.09	$1.509184 \cdot 10^{-5}$	4.09	$8.373657 \cdot 10^{-3}$	4.04
640	$3.125 \cdot 10^{-3}$	$1.584158 \cdot 10^{-3}$	4.01	$2.44727 \cdot 10^{-3}$	4.04	$3.72548 \cdot 10^{-6}$	4.05	$2.070538 \cdot 10^{-3}$	4.04

The second manufactured solution is used to test the streaming limit: the radiation streaming dominates the absorption/re-emission term and evolves at a fast time scale. The exact solutions are the following:

$$\begin{cases} \rho = \sin(x - t) + 2 \\ u = (\sin(x - t) + 2)^{-1} \\ T = 0.5\gamma \\ \epsilon = \sin(x - 1000t) + 2 \end{cases} \quad (15)$$

For this manufactured solution, the cross-sections are still assumed constant and set to the same value 1 cm^{-1} . The final time is $t_{final} = 3 \text{ sh}$. Once again, the L2 error is given in Table 2 for the density, momentum, material total energy and radiation energy density.

Table 2: Convergence study for the second manufactured solution.

DoF	$\Delta t \text{ (sh)}$	ρ	ratio	ρE	ratio	ϵ	ratio	ρu	ratio
20	10^{-1}	$1.4373 \cdot 10^{-2}$	NA	$5.88521 \cdot 10^{-1}$	NA	$3.82001 \cdot 10^{-1}$	NA	$2.354671 \cdot 10^{-3}$	NA
40	$5 \cdot 10^{-2}$	$3.760208 \cdot 10^{-3}$	3.82	$1.4244 \cdot 10^{-1}$	4.13	$1.215 \cdot 10^{-1}$	3.14	$6.138814 \cdot 10^{-4}$	3.84
80	$2.5 \cdot 10^{-2}$	$9.91724 \cdot 10^{-4}$	3.79	$3.2047 \cdot 10^{-2}$	4.44	$3.27966 \cdot 10^{-2}$	3.70	$1.74974 \cdot 10^{-4}$	3.51
160	$1.25 \cdot 10^{-2}$	$2.4455 \cdot 10^{-4}$	4.06	$7.4886 \cdot 10^{-3}$	4.28	$8.38153 \cdot 10^{-3}$	3.91	$3.61297 \cdot 10^{-5}$	4.84
320	$6.25 \cdot 10^{-3}$	$6.280715 \cdot 10^{-5}$	3.89	$1.82327 \cdot 10^{-3}$	4.11	$2.10925 \cdot 10^{-3}$	3.97	$9.03866 \cdot 10^{-6}$	3.99
640	$3.125 \cdot 10^{-3}$	$1.57920 \cdot 10^{-5}$	3.98	$4.50463 \cdot 10^{-4}$	4.05	$5.28472 \cdot 10^{-4}$	3.99	$2.25649 \cdot 10^{-6}$	4.01
1280	$1.5625 \cdot 10^{-4}$	$3.96096 \cdot 10^{-6}$	3.99	$1.12061 \cdot 10^{-4}$	4.02	$1.322268 \cdot 10^{-4}$	3.99	$5.69984 \cdot 10^{-7}$	3.95

For both manufactured solutions the error gets divided by four as the time step Δt and the spatial discretization Δx are reduced by a factor two. Thus, it is concluded that the entropy-based

viscosity method allows the scheme to be second-order accurate when the numerical solution is smooth.

3.2 Numerical solutions:

The purpose of this section is to show that the entropy-based viscosity method (Section 2) can resolve shocks that occur in the radiation-hydrodynamic equations. Multiple test cases are considered with Mach number of 1.05, 1.2, 5 and 50 (ref). All of the simulations are run with 500 cells and a with a constant time step until steady-state. The Courant Friedrichs Lewy (CFL) is specified for each of the test case (even if the scheme employed here is fully implicit, a CFL number can still be computed and is a good reference for comparison against semi-implicit codes). Linear Legendre polynomials and the second-order temporal integrator BDF2 are once again used. For clarity, the step initial conditions of each test case will be given in a table, and plots of the density ($\rho(x)$), the radiation ($\theta(x)$) and material ($T(x)$) temperatures at steady-state will be shown as well as the local viscosity coefficients $\kappa(x)$ and $\kappa_{max}(x)$. The computational domain consists of a 1D slab of thickness L . The initial step is located at x_0 and will be specified for all of test cases. For all of the test cases presented in this paper the cross-sections σ_a and σ_t are assumed constant and set to 853.144 cm^{-1} and 390.711 cm^{-1} , respectively, if not otherwise specified. The heat capacity at constant specific volume is set to $C_v = 0.12348 \text{ jerks}/(g - \text{keV})$.

For the Mach 1.2 simulation, results will be shown when employing the first order viscosity ($\kappa(x, t) = \kappa_{max}(x, t)$). The objective, here, is to show the benefits of using a second-order viscosity coefficients.

It remains, now, to specify the type of boundary conditions employed at the inlet and outlet. The Euler equations and radiation equation are considered independently since the latest one is parabolic. At the inlet, the flow is supersonic and therefore none physical information exits the system. Thus, Dirichlet boundary condition can be used. At the outlet, the flow become subsonic which requires a particular treatment. Following the work from [21], a static boundary condition is implemented. Only the back pressure is provided and the other variables are computed using the characteristic equations. For the radiation equation, the treatment of the boundary condition is easier and a simple void boundary conditions is used for both the inlet and outlet boundaries.

3.2.1 An equilibrium diffusion test:

For this test, the inlet Mach number is set to 1.05. The radiation field and material are in equilibrium. The following initial conditions were used: For this test, the computational domain

Table 3: Initial conditions for Mach 1.05.

	left	right
$\rho \text{ (g/cm)}$	1.	1.0749588
$u \text{ (cm/sh)}$	0.1228902	0.1144127
$T \text{ (keV)}$	0.1	0.1049454
$\epsilon \text{ (jerks/cm}^3\text{)}$	$1.372 \cdot 10^{-6}$	$1.6642117 \cdot 10^{-6}$

had a size $L = 0.030 \text{ cm}$ and the initial step was located in the middle at $x_0 = 0.015 \text{ cm}$. The numerical solutions at steady-state are given in Fig. 1, Fig. 2 and Fig. 3. The solution was run with $CFL = 10$.

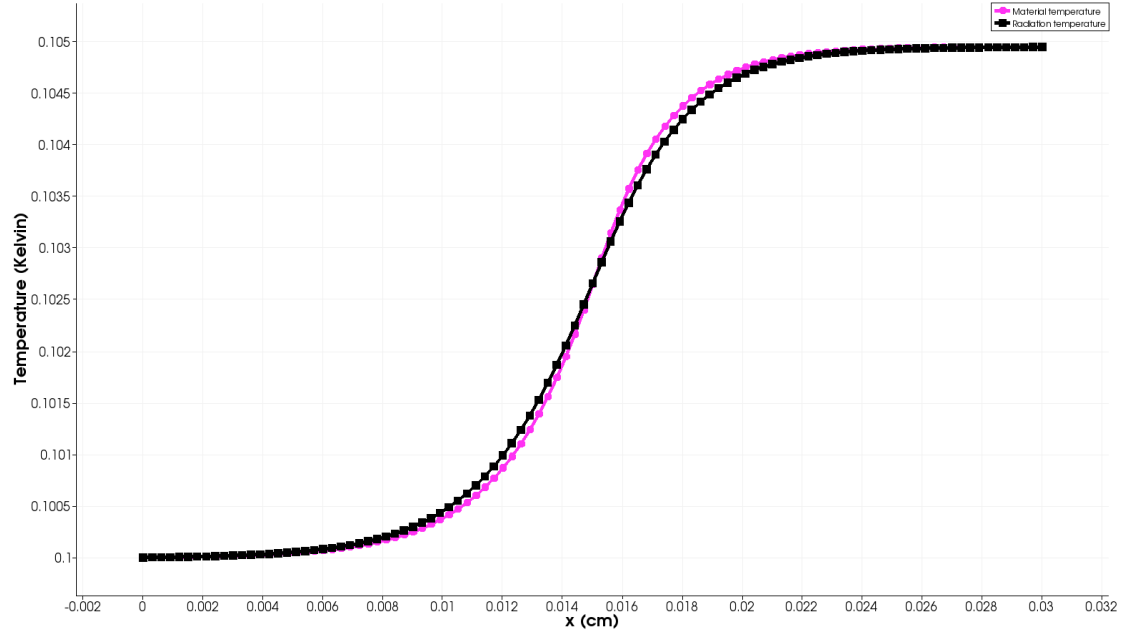


Figure 1: Material (square) and radiation (circle) temperature profiles at steady-state for Mach 1.05 test.

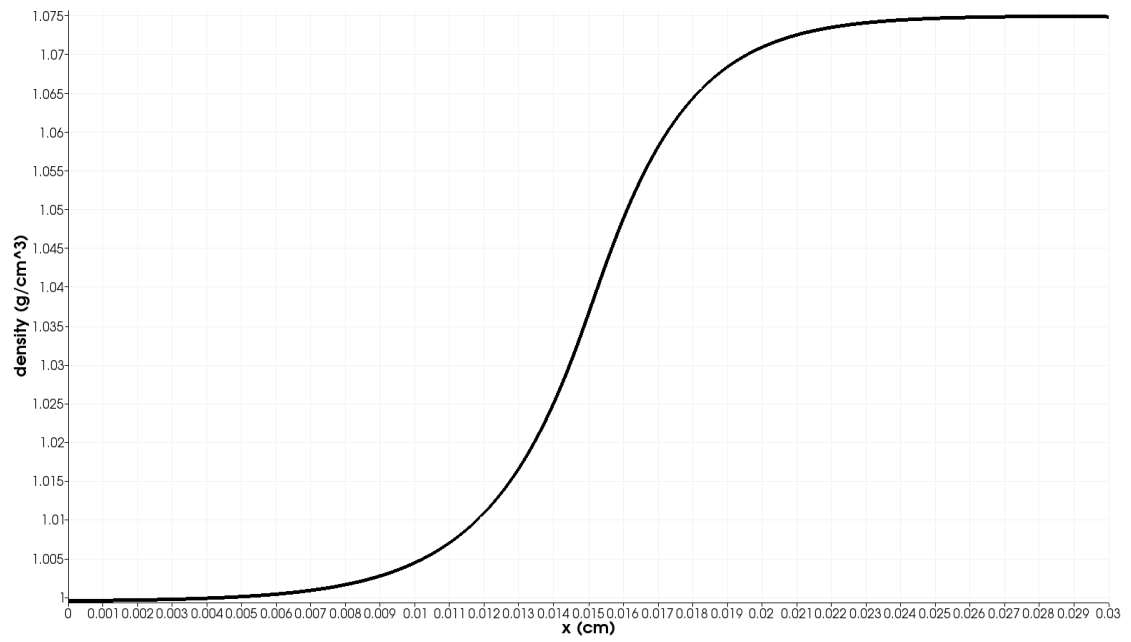


Figure 2: Material density profile at steady-state for Mach 1.05 test.

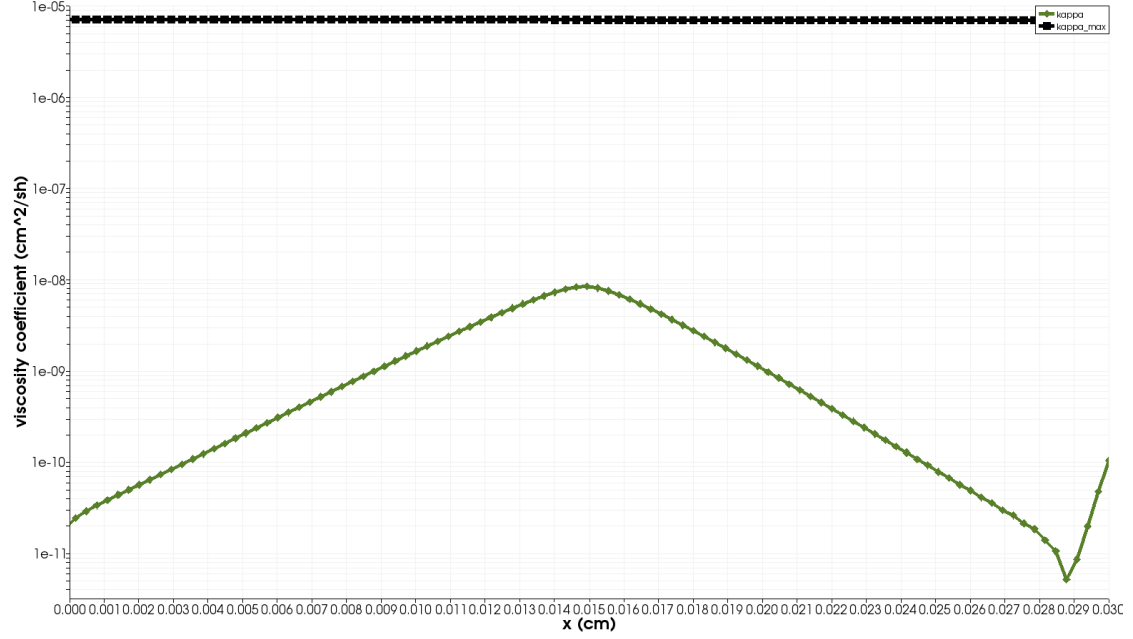


Figure 3: First-order viscosity κ_{max} (square) and second-order viscosity κ (circle) profiles at steady-state for Mach 1.05 test (logarithm scale).

The energy transfer between the material and radiation fields is not large enough to form a shock in the material. Thus, all of the material variables are smooth (Fig. 1 and Fig. 2) as well as the radiation temperature θ . Because of the smoothness of the solution, the viscosity coefficient κ is three order of magnitude smaller than the first-order viscosity coefficient κ_{max} (Fig. 3).

3.2.2 A 1.2 Mach hydrodynamic shock:

In this test, the material experiences a shock and the radiation energy density remains smooth. The initial conditions corresponding to the Mach number of 1.2 at the inlet are the following.

Table 4: Initial conditions for Mach 1.2.

	left	right
ρ (g/cm)	1.	1.0749588
u (cm/sh)	0.1405588	0.1083456
T (keV)	0.1	0.1194751
ϵ (jerk/cm ³)	$1.372 \cdot 10^{-6}$	$2.7955320 \cdot 10^{-6}$

The slab thickness is set to $L = 1 \cdot 10^{-3}$ cm and the initial step was located at $x_0 = 0.0005$ cm.

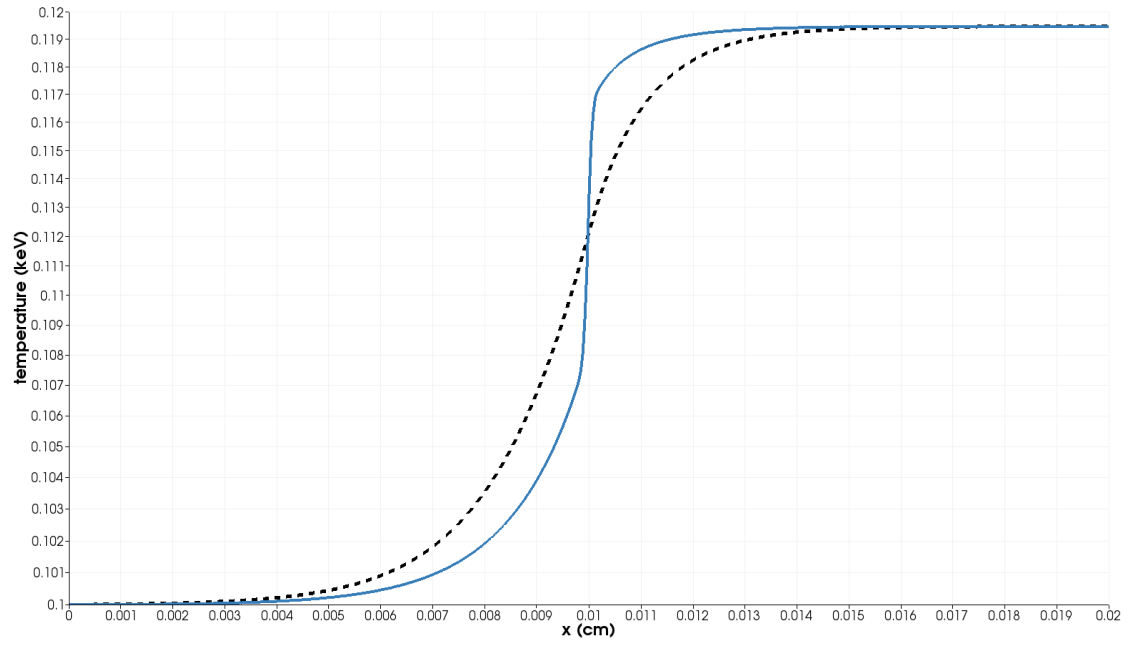


Figure 4: Material (solid line) and radiation (dashed line) temperature profiles at steady-state for Mach 1.2 test.

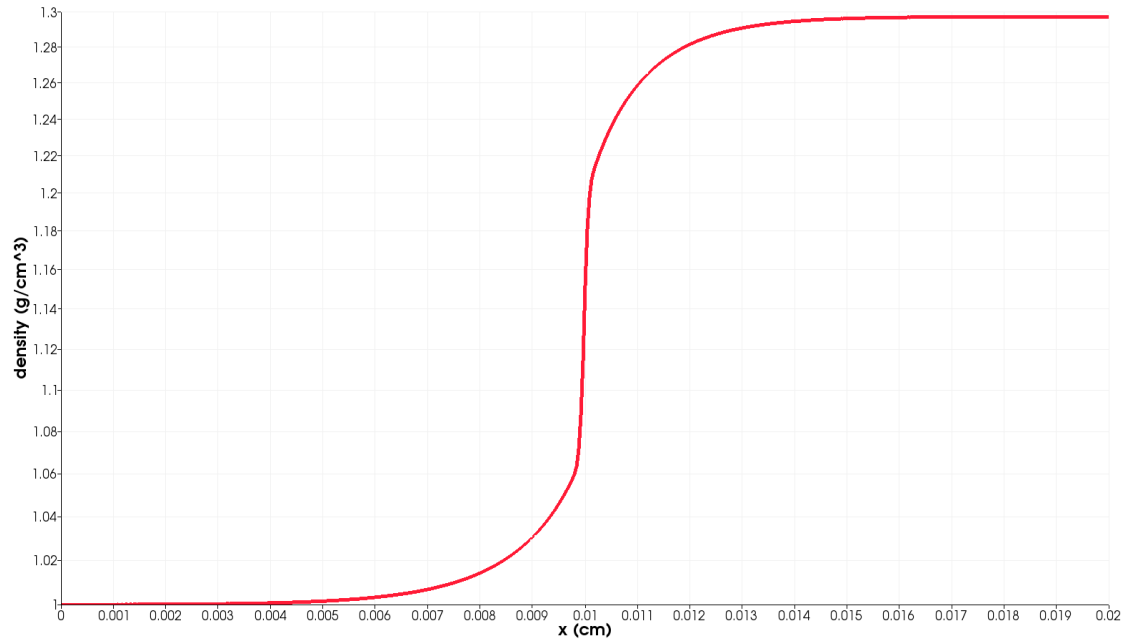


Figure 5: Material density profile at steady-state for Mach 1.2 test.

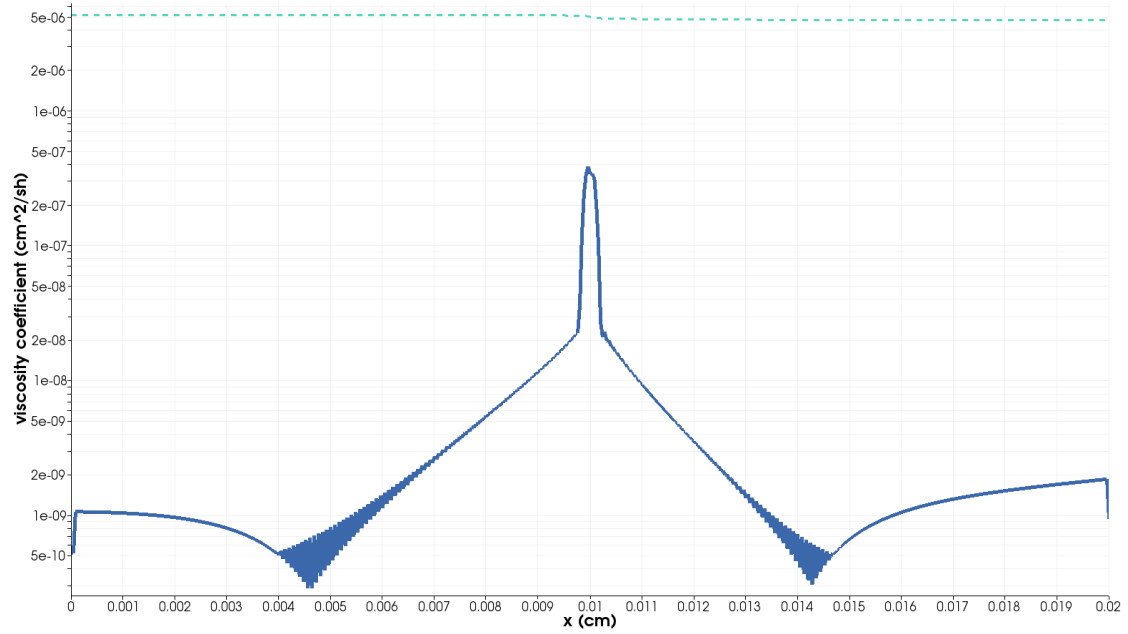


Figure 6: First-order viscosity κ_{max} (dashed line) and second-order viscosity κ (solid line) profiles at steady-state for Mach 1.2 test (logarithm scale).

3.2.3 A Mach 2 shock:

The Mach 2 shock has two features: a hydrodynamic shock and a isothermal sonic point (ISP), which make it interesting for testing the robustness of the entropy-based viscosity method. The initial conditions are specified in Table 5:

Table 5: Initial conditions for Mach 2.

	left	right
ρ (g/cm)	1.	1.0749588
u (cm/sh)	0.1405588	0.1083456
T (keV)	0.1	0.1194751
ϵ (jerks/cm ³)	$1.372 \cdot 10^{-6}$	$2.7955320 \cdot 10^{-6}$

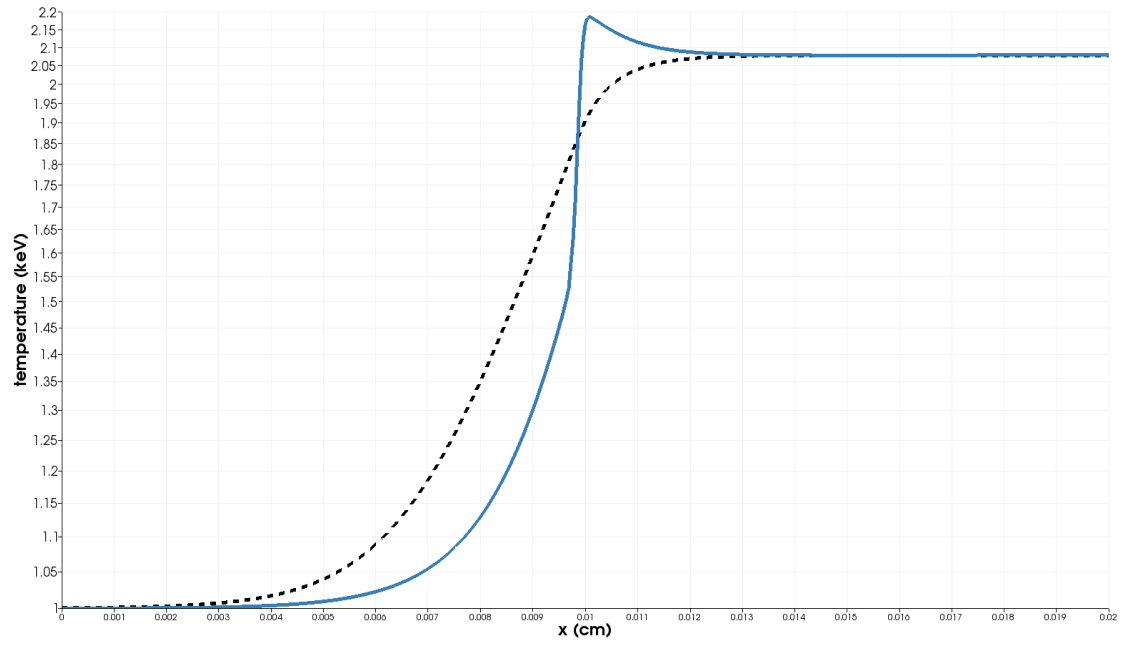


Figure 7: Material (solid line) and radiation (dashed line) temperature profiles at steady-state for Mach 2 test.

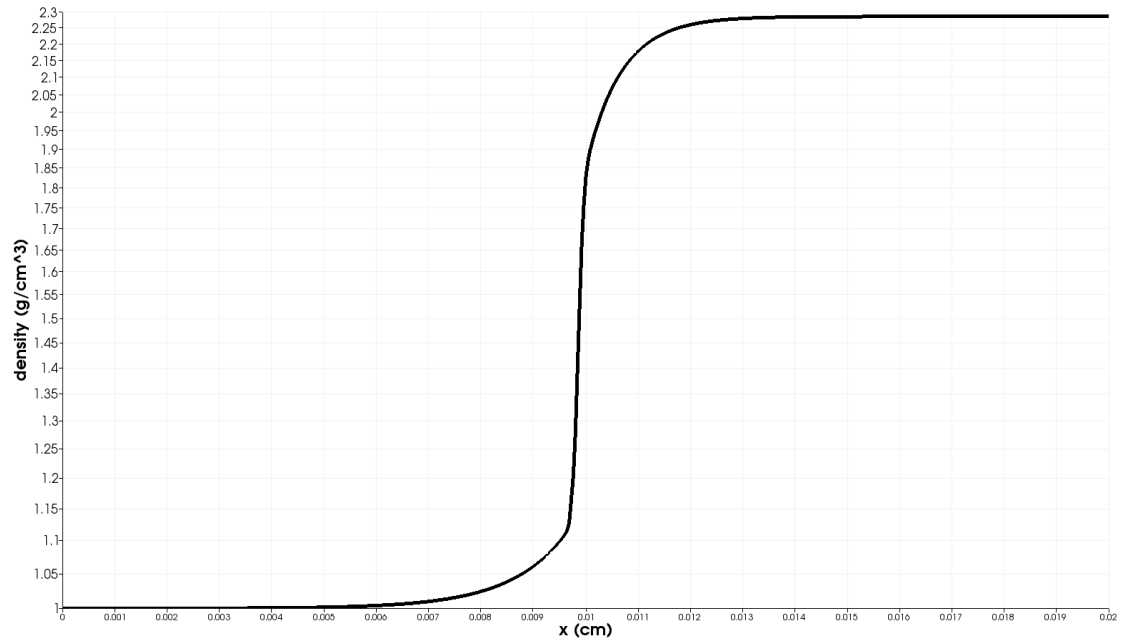


Figure 8: Material density profile at steady-state for Mach 1.2 test.

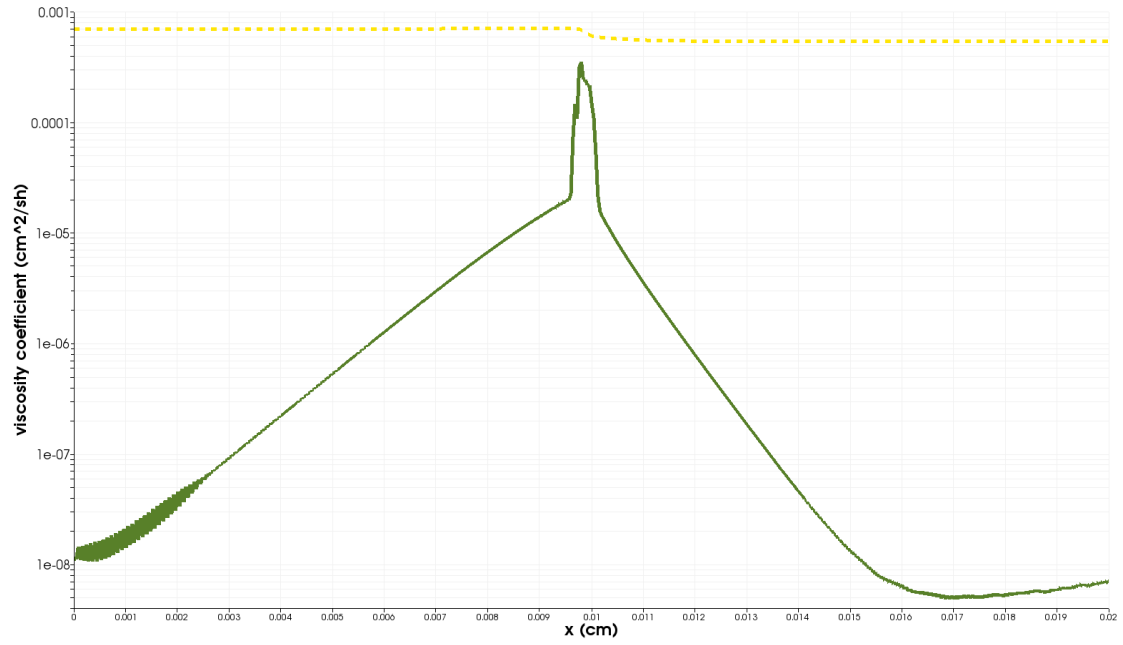


Figure 9: First-order viscosity κ_{max} (dashed line) and second-order viscosity κ (solid line) profiles at steady-state for Mach 2 test (logarithm scale).

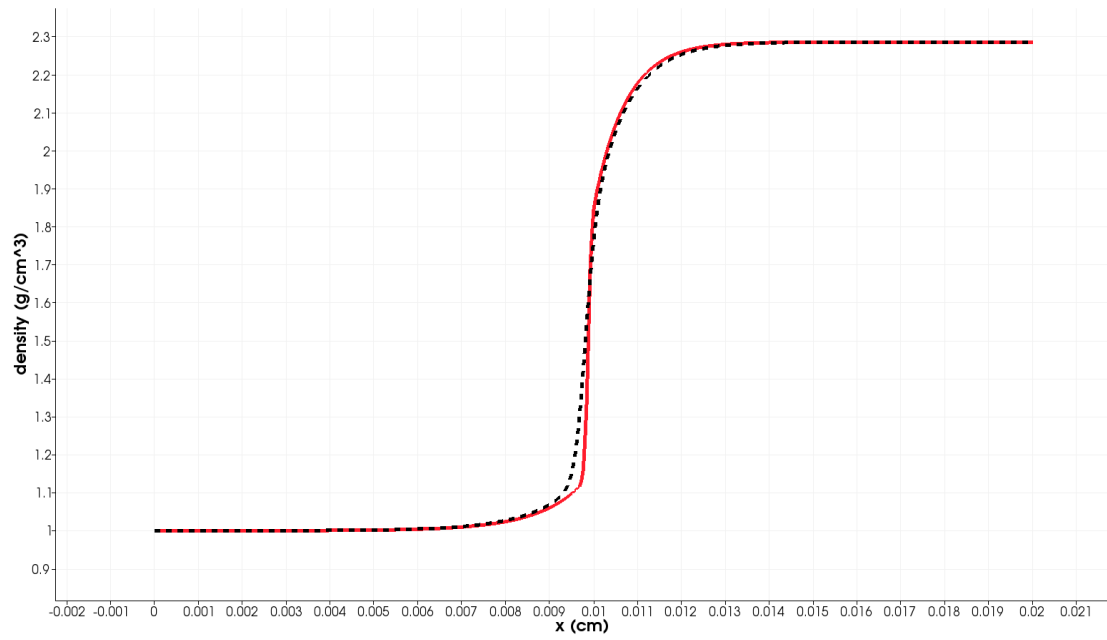


Figure 10: Comparison between material density run with second-order and first-order viscosity: material density with second-order viscosity (solid line) and material density with first-order viscosity (dashed line).

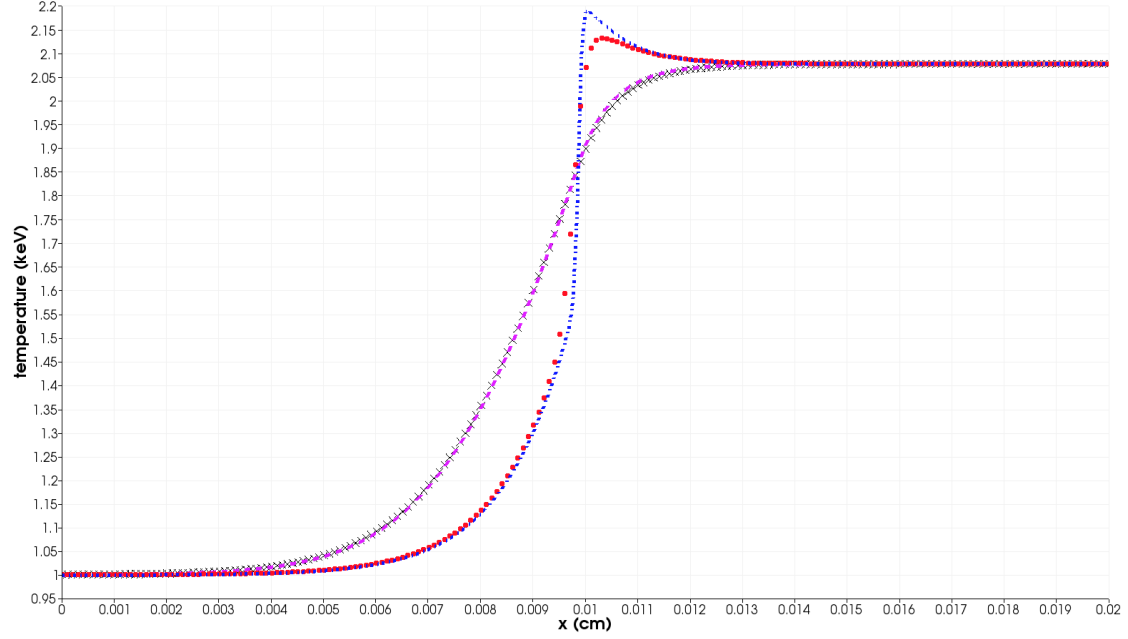


Figure 11: Comparison between the material and radiation temperatures run with the second order and first order viscosity coefficient: radiation temperature with second-order viscosity (dashed line), radiation temperature with first-order viscosity (cross), material temperature with second-order viscosity (dot dashed line) and material temperature with first-order viscosity (circle).

3.2.4 Mach 5 shock:

Table 6: Initial conditions for Mach 5.

	left	right
ρ (g/cm)	1.	1.0749588
u (cm/sh)	0.1405588	0.1083456
T (keV)	0.1	0.1194751
ϵ ($jerk/cm^3$)	$1.372 \cdot 10^{-6}$	$2.7955320 \cdot 10^{-6}$

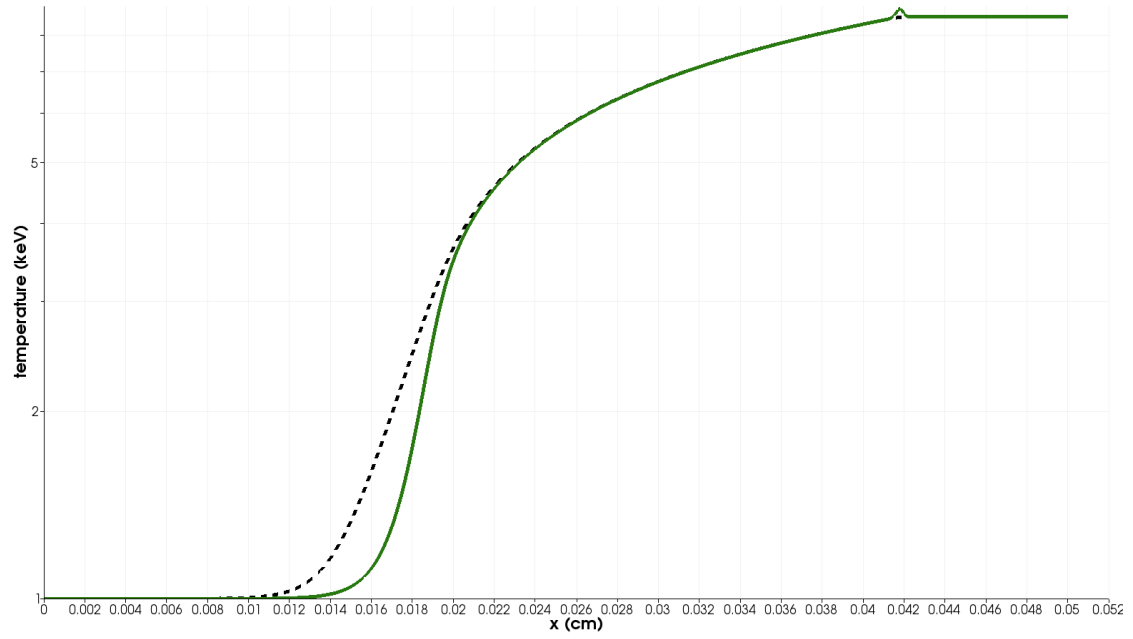


Figure 12: Material (solid line) and radiation (dashed line) temperature profiles at steady-state for Mach 5 test.

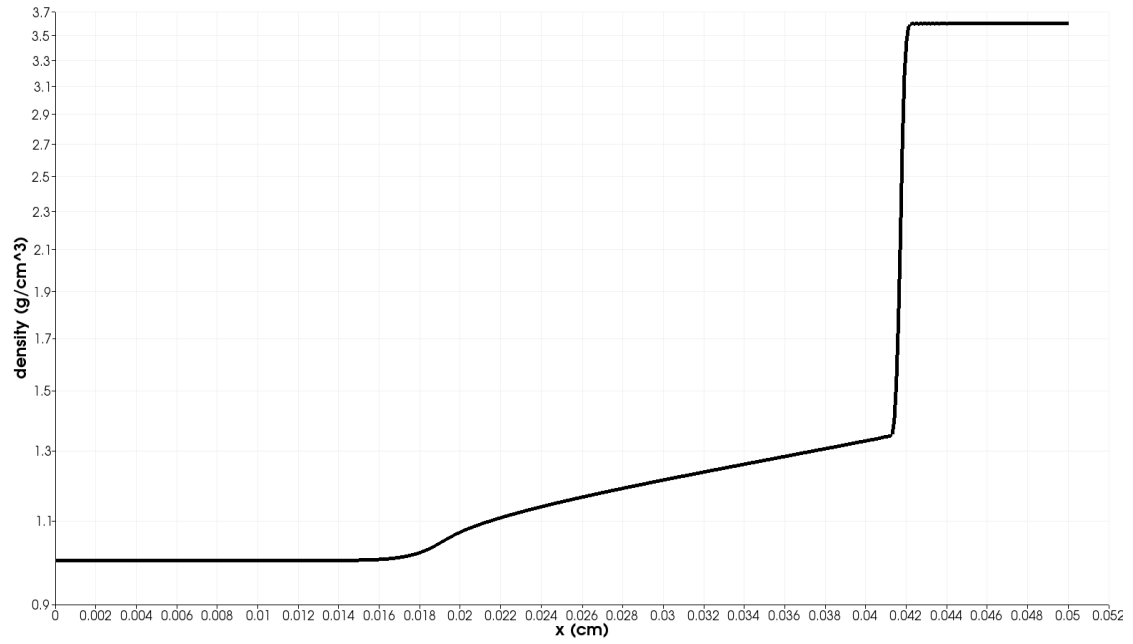


Figure 13: Material density profile at steady-state for Mach 5 test.

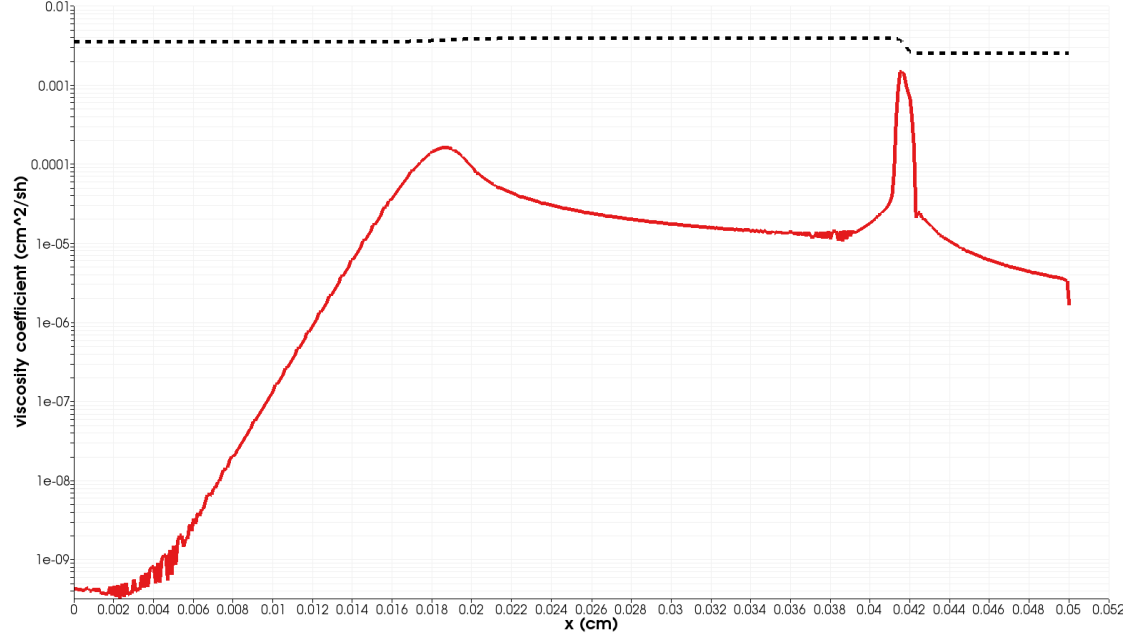


Figure 14: First-order viscosity κ_{max} (dashed line) and second-order viscosity κ (solid line) profiles at steady-state for Mach 5 test (logarithm scale).

3.2.5 Mach 50 shock:

Table 7: Initial conditions for Mach 50.

	left	right
ρ (g/cm)	1.	6.5189217
u (cm/sh)	585.6620	89.84031
T (keV)	1.0	85.51552
ϵ (jerks/cm ³)	$1.372 \cdot 10^{-2}$	$7.33726 \cdot 10^5$

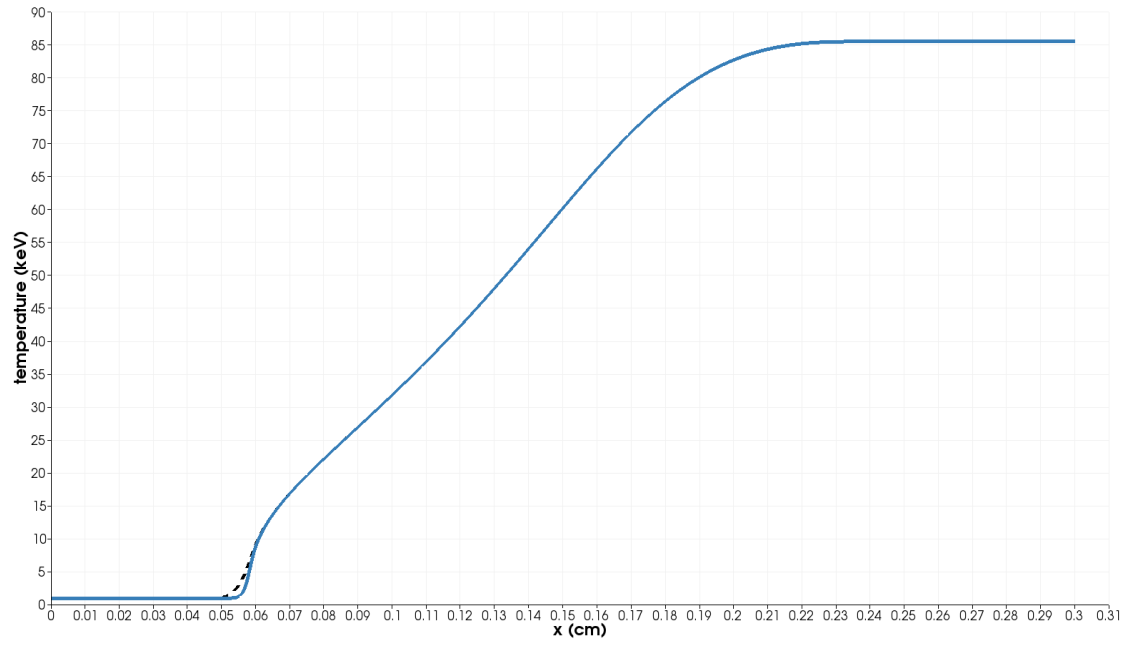


Figure 15: Material (solid line) and radiation (dashed line) temperature profiles at steady-state for Mach 50 test.

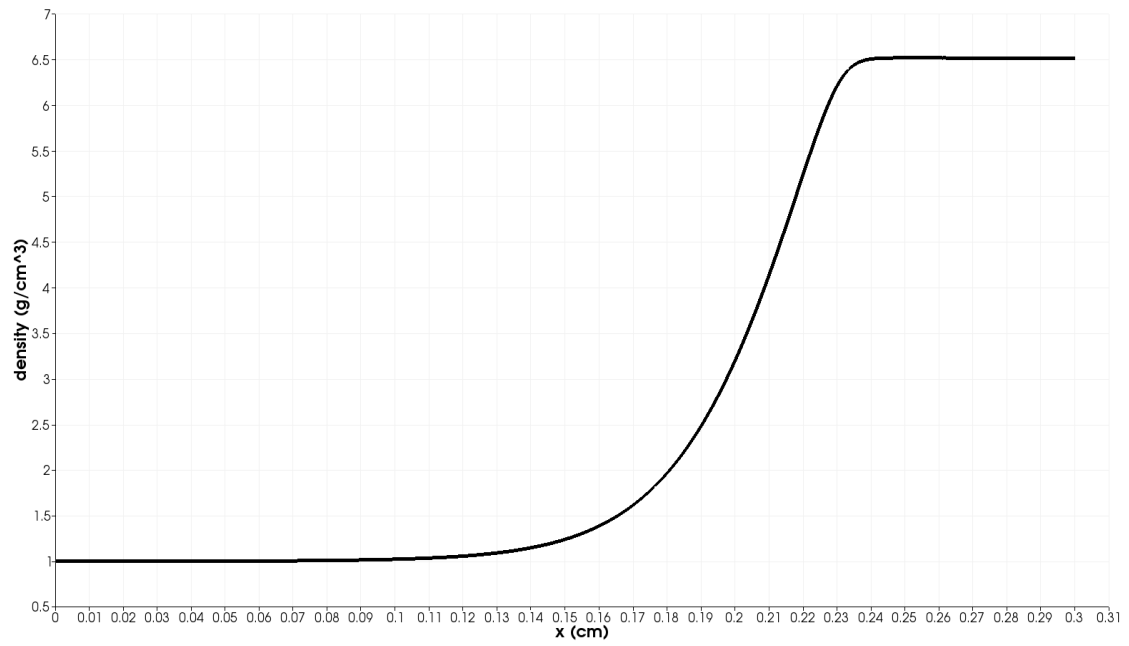


Figure 16: Material density profile at steady-state for Mach 50 test.

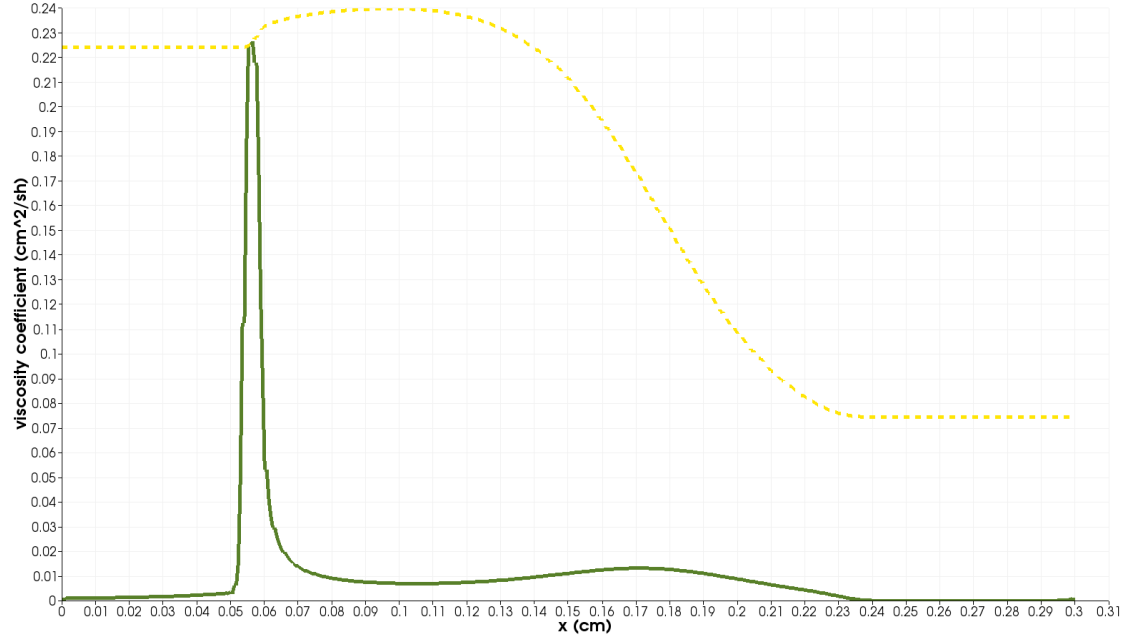


Figure 17: First-order viscosity κ_{max} (dashed line) and second-order viscosity κ (solid line) profiles at steady-state for Mach 50 test (logarithm scale).

4 Conclusion:

A Proof of the entropy minimum principle for the radiation-hydrodynamic equations with dissipative terms:

In this appendix, the entropy minimum principle for the system of equations given in Eq. (7) is proved. This proof is inspired of [19] that details the steps that lead to the derivation of the dissipative terms for the multi-D Euler equations by using the entropy minimum principle theorem.

We start with the system given in Eq. (3) by adding dissipative terms to each equation as follows:

$$\begin{cases} \frac{d\rho}{dt} + \rho\partial_x u = \partial_x f \\ \partial_t(\rho u) + \partial_x(\rho u^2 + P + \frac{\epsilon}{3}) = \partial_x g \\ \partial_t(\rho E) + \partial_x[u(\rho E + P)] = \partial_x(h + ug) \\ \partial_t\epsilon + u\partial_x\epsilon + \frac{4}{3}\epsilon\partial_x u = \partial_x l \end{cases} \quad (16)$$

where f , g , h and l are dissipative terms to determine. Eq. (16) is now recast as a function of the primitive variables (ρ, u, e, ϵ) to yield:

$$\begin{cases} \frac{d\rho}{dt} + \rho\partial_x u = \partial_x f \\ \rho\frac{du}{dt} + \partial_x(P + \frac{\epsilon}{3}) = \partial_x g - u\partial_x f \\ \rho\frac{de}{dt} + P\partial_x u = \partial_x h + g\partial_x u + (0.5u^2 - e)\partial_x f \\ \frac{d\epsilon}{dt} + \frac{4}{3}\epsilon\partial_x u = \partial_x l \end{cases} \quad (17)$$

The right-hand side of the internal energy equation can be simplified by carefully choosing the dissipative terms g and h as follows: $h = \tilde{h} - 0.5u^2 f$ and $g = \rho\mu\partial_x u + uf$. Using these definitions, the system of equation given in Eq. (18) yields:

$$\begin{cases} \frac{d\rho}{dt} + \rho\partial_x u = \partial_x f \\ \rho\frac{du}{dt} + \partial_x(P + \frac{\epsilon}{3}) = \partial_x g - u\partial_x f \\ \rho\frac{de}{dt} + P\partial_x u = \rho\mu(\partial_x u)^2 + \partial_x \tilde{h} - e\partial_x f \\ \frac{d\epsilon}{dt} + \frac{4}{3}\epsilon\partial_x u = \partial_x l \end{cases} \quad (18)$$

where $\mu \geq 0$ is a dissipative coefficient.

This system of equation admits an entropy s function of the density ρ , the internal energy e and the radiate energy density ϵ . In order to prove the entropy minimum principle, a partial differential equation (PDE) verified by the entropy is needed. This PDE is referred to as an entropy residual $D_e(x, t)$ and can be obtained by combination of the equations given in Eq. (18). This process is motivated by the following observation

$$\partial_\alpha s = \partial_\rho s \partial_\rho + \partial_e s \partial_e + \partial_\epsilon s \partial_\epsilon, \quad (19)$$

which holds for any independent variable (x, t) . It is also required to define the dissipative terms \tilde{h} , f and l . The following definitions are chosen:

$$\begin{cases} f &= \kappa\partial_x \rho \\ \tilde{h} &= \kappa\partial_x(\rho e) \\ l &= \kappa\partial_x \epsilon \end{cases} \quad (20)$$

where κ is another dissipative coefficient.

Thus, using Eq. (18) and Eq. (19) along with the definition of the dissipative terms, a PDE verified by the entropy s is obtained:

$$\frac{ds}{dt} + \underbrace{\left(P\partial_e s + \rho^2\partial_\rho s + \frac{4}{3}\rho\epsilon\partial_\epsilon s\right)}_{(a)} \partial_x u = \partial_x(\rho\kappa\partial_x s) + \underbrace{\kappa\partial_e s \partial_x s}_{(b)} - \underbrace{\rho\kappa \underbrace{XAX^t}_{(b)} + s_e \rho\mu(\partial_x u)^2}_{(c)} \quad (21)$$

where X is a row vector defined as $X = (\rho, e, \epsilon)$ and A is a 3 by 3 symmetric matrix with the following definition:

$$A = \begin{bmatrix} \partial_\rho (\rho^2 \partial_\rho s) & \partial_{\rho,e} s & \partial_\rho (\rho \partial_\epsilon s) \\ \partial_{\rho,e} s & \partial_{e,e} s & \partial_{e,\epsilon} s \\ \partial_\rho (\rho \partial_\epsilon s) & \partial_{e,\epsilon} s & \partial_{\epsilon,\epsilon} s \end{bmatrix} \quad (22)$$

In order to show that an entropy minimum principle holds, the sign of the terms (a), (b) and (c) are studied.

To determine the sign of term (a), it is assumed that $P \partial_e s + \rho^2 \partial_\rho s + \frac{4}{3} \rho \epsilon \partial_\epsilon s = 0$. This assumption is motivated by the following statement: in order to have a sign for the term (a), it would require $P \partial_e s + \rho^2 \partial_\rho s + \frac{4}{3} \rho \epsilon \partial_\epsilon s$ to be proportional to the $\partial_x u$. The thermodynamic variables cannot be function of the material velocity of its derivative under a non-relativistic assumption. Such a statement would be no longer true when dealing with relativistic equation of states.

The term (b), XAX^t , is a quadratic form and its sign is determined by simply looking at the positiveness of the matrix A [16]. For the case under consideration, it is needed to prove that the matrix A is negative-definite which is equivalent to the three following inequalities:

$$\begin{cases} A_1 \geq 0 \\ A_2 \leq 0 \\ A_3 = A \geq 0 \end{cases} \quad (23)$$

where A_k is the k^{th} order leading principle minor. Determining the sign of the last inequality that corresponds to the determinant of the 3 by 3 matrix A can be difficult. The ideal case would be to zero the off-diagonal terms of the last row and column so that the determinant of A becomes simpler. Under this assumption, the determinant of A can be easily computed. This can be achieved by assuming the following form of the entropy function $s(\rho, e, \epsilon)$:

$$s(\rho, e, \epsilon) = \tilde{s}(\rho, e) + \frac{\rho_0}{\rho} \hat{s}(\epsilon). \quad (24)$$

where \tilde{s} and \hat{s} are two functions whom properties will be given along this derivation. The constant ρ_0 is used for dimension purpose and can be set to one. Thus, using the expression of the entropy given in Eq. (24), the matrix A yields a block matrix:

$$A = \begin{bmatrix} \partial_\rho (\rho^2 \partial_\rho \tilde{s}) & \partial_{\rho,e} \tilde{s} & 0 \\ \partial_{\rho,e} \tilde{s} & \partial_{e,e} \tilde{s} & 0 \\ 0 & 0 & \rho^{-1} \partial_{\epsilon,\epsilon} \hat{s} \end{bmatrix}$$

Proving that the matrix A is negative-definite is now straightforward by computing and looking at the sign of the leading principal minors:

$$\begin{cases} A_1 = \partial_\rho (\rho^2 \partial_\rho \tilde{s}) \leq 0 \\ A_2 = \partial_\rho (\rho^2 \partial_\rho \tilde{s}) \partial_{e,e} \tilde{s} - (\partial_{\rho,e} \tilde{s})^2 \geq 0 \\ A_3 = \rho^{-1} \partial_{\epsilon,\epsilon} \hat{s} A_2 \leq 0 \end{cases} \quad (25)$$

which is easily achieved when assuming that the function $-\tilde{s}$ and $-\hat{s}$ are convex. Thus, the sign of (b) is now known.

It remains to determine the sign of the term (c) $= s_e \rho \mu (\partial_x u)^2$. The density ρ and the viscosity coefficient μ are both positive: the latest by definition, and proof of positivity of the density can be found in [19]. Then, only the sign of s_e is still unknown but can be determined by studying (a). It is assumed earlier in this appendix that $P \partial_e s + \rho^2 \partial_\rho s + \frac{4}{3} \rho \epsilon \partial_\epsilon s = 0$. This equation is now

recast and split into two equations using Eq. (24) and the method of separation of variables to yield:

$$P\tilde{s}_e + \rho^2\tilde{s}_\rho = A \text{ and } \hat{s} - \frac{4\epsilon}{3}\hat{s}_\epsilon = A$$

where A is a constant to determine. It is chosen to set $A = 0$ so that the two physics get decoupled. But more important is, that it allows us to reconnect to the result derived in [19]: $P\tilde{s}_e + \rho^2\tilde{s}_\rho = 0$. Then, following [19], a definition for \tilde{s}_e and \tilde{s}_ρ is obtained:

$$\begin{cases} s_e = \tilde{s}_e = T^{-1} \\ \tilde{s}_\rho = -\frac{P}{\rho^2}\tilde{s}_e \end{cases}$$

where T is the material temperature which ensures positivity of s_e . Then, (c) is positive.

From the above results, the entropy minimum principle follows, so that the sign of the entropy residual is known:

$$\boxed{\partial_t s + u\partial_x s \geq 0} \quad (26)$$

Remark A.1. By assuming $A = 0$, an expression for the \hat{s} can be derived by solving the ODE, $\hat{s} - \frac{4\epsilon}{3}\hat{s}_\epsilon = 0$, which yields: $\hat{s}(\epsilon) = B \exp\left(\frac{4\epsilon^2}{3}\right)$, where B is a constant. The sign of B is determined by using the condition, $\partial_{\epsilon,\epsilon}\hat{s} \leq 0$ derived above, so that $B \leq 0$.

Remark A.2. The viscous regularization derived in this appendix, has two viscosity coefficients μ and κ . For the purpose of this paper, the two viscosity coefficients are set equal. Under this assumption, the above viscous regularization is equivalent to the parabolic regularization.

References

- [1] *Upwind and high-resolution schemes*, Hussaini MY, van Leer B, Van Rosendale J, Berlin: Springer, 1997.
- [2] *Entropy viscosity method for nonlinear conservation laws*, Jean-Luc Guermond, R. Pasquetti, B. Popov, J. Comput. Phys., 230 (2011) 4248-4267.
- [3] *Entropy Viscosity Method for High-Order Approximations of Conservation Laws*, J-L. Guermond, R. Pasquetti, Lecture Notes in Computational Science and Engineering, Springer, Volume 76, (2011) 411-418.
- [4] *Numerical methods for conservation laws*, LeVeque RJ, Lectures in Mathematics, Basel: Birkhauser, 1990
- [5] *An Analysis of the Hyperbolic Nature of the Equations of Radiation Hydrodynamics*, Dinshaw S. Balsara, J. Quant. Spectrosc. Radiat. Transfer, Vol. 61, No. 5, pp. 617-627, 1999.
- [6] *Coupling radiation and hydrodynamics*, Lowrie RB, Morel JE, Hittinger JA, 521 (1), 432-50 (1999).
- [7] *Numerical simulations for radiation hydrodynamics. I. Diffusion limit* Dai W, Woodward PR, J. Comput Phys (1998), 142, 182-207.
- [8] *A diffusion synthetic acceleration method for the SN equations with discontinuous finite element space and time differencing*, T.A. Wareing, J.E. Morel, J.M. McGhee, Proceedings of the International Conference on Mathematics and Computation, Reactor Physics and Environmental Analysis in Nuclear Applications, Madrid, Spain, September 27-30, vol. 1, pp. 45-44.
- [9] *Solving ordinary differential equations II*, Second Revised ed., Springer Series in Computational Mathematics, Springer, New York, 2002.
- [10] *Nonlinear variants of the TR-BDF2 method for thermal radiative diffusion*, Jarrods D. Edwards, Jim E. Morel, Dana A. Knoll, Journal of Computational Physics, 230 (2011), 1198-1214.
- [11] *Riemann Solvers and numerical methods for fluid dynamics*. E.F. Toro, 2nd Edition, Springer.
- [12] *Implementation of the entropy viscosity method with the discontinuous Galerkin method*, Valentin Zingan, Jean-Luc Guermond, Jim Morel, Bojan Popov, Volume 253, 1 January 2013, Pages 479-490
- [13] *E. Tadmor. A minimum entropy principle in the gas dynamics equations*, Appl. Numer. Math., 2(3-5):211-219, 1986.
- [14] *Issues with high-resolution Godunov methods for radiation hydrodynamics*, R.B. Lowrie, J.E. Morel, Journal of Quantitative Spectroscopy & Radiative Transfer, 69, 475-489 (2001).
- [15] *Weak solutions of nonlinear hyperbolic equations and their numerical computation*, P. Lax, Comm. Pure Appl. Math., 7:159-193, 1954.

- [16] *Numerical approximations of hyperbolic systems of conservation laws*, E. Godlewski and P.-A. Raviart, volume 118 of Applied Mathematical Sciences. Springer-Verlag, New York, 1996. ISBN 0-387-94529-6.
- [17] *Second-Order Discretization in Space and Time for Radiation Hydrodynamics*, Jarrod D. Edwards, Jim E. Morel, Robert B. Lowrie, International Conference on Mathematics and Computational Methods Applied to Nuclear Science & Engineering (M&C 2013), Sun Valley, Idaho USA, May 5-9, American Nuclear Society, LaGrange Park, IL (2013).
- [18] *Numerical Schemes for Hyperbolic Conservation Laws with Stiff Relaxation Terms*, Shi Jin and C. David Levermore, Journal of Computational Physics, 126, 449-467 (1996).
- [19] *Viscous regularization of the Euler equations and entropy principles*, Jean-Luc Guermond and Bojan Popov, under review.
- [20] *A parallel computational framework for coupled systems of nonlinear equations*, D. Gaston, C. Newsman, G. Hansen and D. Lebrun-Grandie, Nucl. Eng. Design, vol 239, pp 1768-1778, 2009.
- [21] *The discrete equation method (DEM) for fully compressible, two-phase flows in ducts of spatially varying cross-section*. R.Berry, R.Saurel, O. LeMetayer, Nuclear Engineering and Design 240 (2010) 3797-3818.